Mountain permafrost dynamics within a recently exposed glacier forefield inferred by a combined geomorphological, geophysical and photogrammetrical approach

C. Kneisel[1]* and A. Kääb[2]
[1] *Department of Physical Geography, University of Würzburg, Würzburg, Germany*
[2] *Department of Geosciences, University of Oslo, Oslo, Norway*

*Correspondence to:
Dr. Christof Kneisel, Department of Physical Geography, University of Würzburg, D-97074 Würzburg, Germany.
E-mail: kneisel@uni-wuerzburg.de*

Abstract

Geomorphological observations, geoelectrical soundings and photogrammetric measurements of surface movement on the Muragl glacier forefield were used to obtain an integrative analysis of a highly complex glacial and periglacial landform consisting of a push moraine, creeping permafrost and permafrost-free glacial till in close proximity. Electrical resistivity tomography is considered as an important multifunctional geophysical method for research in periglacial permafrost related environments. Joint application with measurements of surface displacements offers a promising tool for investigating periglacial landforms related to ice-rich permafrost for a more comprehensive characterization of permafrost characteristics and geomorphological interpretation of periglacial morphodynamics. The patchy permafrost distribution pattern described in this paper is determined by several factors, including the sediment characteristics, the snow cover distribution and duration, the aspect and the former glacier distribution and thermal regime. Recent and modern permafrost dynamics within the glacier forefield comprise aggradation, degradation and permafrost creep. Copyright © 2007 John Wiley & Sons, Ltd.

Keywords: mountain permafrost dynamics; glacier–permafrost interaction; permafrost creep; electrical resistivity imaging; photogrammetry

Introduction

In cold mountains, polythermal glaciers and permafrost often exist in close proximity, where climate conditions transit between wet-maritime and dry-continental regimes. Under such conditions a regional decrease in glacier size is often accompanied by an increase in the occurrence of discontinuous permafrost and related periglacial and glacial landforms such as rock glaciers and push moraines (cf. Haeberli, 1983; Kneisel *et al.*, 2000; Maisch *et al.*, 2003; Kääb and Kneisel, 2006). In this paper the term push moraine is used in its strict sense as a glaciotectonically deformed permafrost landform.

The massive retreat of small mountain glaciers at high altitudes since the last maximum glacier extent (Little Ice Age, LIA, around AD 1850 in the European Alps) situated in areas with permafrost favourable conditions, uncovers forefields, some of which contain thick coarse deposits of glacial and periglacial origin – favourable prerequisites for permafrost aggradation and creep. The local permafrost distribution pattern within these recently deglaciated glacier forefields is influenced by several factors, including the sediment characteristics, the snow cover distribution and duration, the aspect and the former glacier distribution and thermal regime. Perennially frozen ground in areas deglaciated since the Little Ice Age may represent either formerly subglacial permafrost preserved or developed underneath cold surface ice, or permafrost that has formed since the disappearance of temperate surface ice (Kneisel, 2003a). Questions arise concerning the extent to which potentially pre-existing permafrost was influenced by overriding during the LIA glacier advances, and the extent and rate to which permafrost and ground ice can build up, or recover, after ground exposure to the atmosphere due to glacier retreat.

This paper presents an assessment of recent permafrost dynamics using a combined geomorphological, geophysical and photogrammetrical approach. So far, geomorphological mapping, ground surface temperature measurements

(e.g. bottom temperature of the winter snow cover, BTS) and geophysical soundings have been used to investigate thermal conditions and permafrost occurrences in recently exposed glacier forefields and to infer glacier–permafrost interactions (Haeberli, 1983, 1992; Kneisel, 1998, 1999, 2003a, 2004; Lugon *et al.*, 2004; Delaloye, 2004; Reynard *et al.*, 2003). Here digital photogrammetric measurements of surface displacement are applied to the investigated glacier forefield and results are compared with geoelectrical surveys. The combination of measured surface displacement fields with geophysical surveys of subsurface conditions has been shown to be a successful concept for investigating creeping mountain permafrost (Vonder Mühll and Schmid, 1993; Berthling *et al.*, 1998; Hoelzle *et al.*, 1998; Potter *et al.*, 1998; Konrad *et al.*, 1999; Isaksen *et al.*, 2000; Ikeda *et al.*, 2003; Bucki and Echelmeyer, 2004; Bucki *et al.*, 2004; Lambiel and Delaloye, 2004; Kääb and Kneisel, 2006).

This contribution illustrates the potential use of the applied methodologies and combined interpretation of their results for periglacial geomorphology, and significantly extends the earlier study (Kääb and Kneisel, 2006) by introducing a larger number of and more recent findings from the electrical resistivity imaging, allowing for more detailed interpretation and conclusions. The two-dimensional geoelectrical surveys were performed in 2002 and 2004 to delineate the small-scale present-day permafrost occurrence and characteristics. For the latter surveys the locations of the profiles were chosen in those areas of the forefield with significant surface displacement rates. For interpretation of the photogrammetric displacement measurements a coherent surface velocity field is viewed as a proxy for frozen debris with a slope steep enough, and with an ice content high and long-lasting enough to allow for significant ductile deformation of the material. Hereby, inferences can be made as to the recent and present-day permafrost dynamics and the interplay between ground ice content and slope deformation. Furthermore, the combined approach allows a better understanding of the Holocene and LIA landscape evolution influenced by complex glacier–permafrost interactions, enabling a genetic differentiation of various periglacial permafrost creep landforms.

Study Site

The study site is situated in the Upper Engadine, eastern Swiss Alps, in the vicinity of St. Moritz. The regional climate can be described as continental, with fairly low precipitation and comparatively high temperature amplitude. Only very small cirque glaciers, glacierets and perennial snow/ice patches exist today. Periglacial morphodynamics clearly predominate over glacial morphodynamics. Numerous rock glaciers are obvious geomorphological indicators of the discontinuous distribution of alpine permafrost.

The investigated glacier forefield (46°30′15″ N, 9°56′30″ E) is located in the Muragl valley, close to the well investigated currently active Muragl rock glacier (Kääb and Vollmer, 2000; Arenson *et al.*, 2002; Vonder Mühll *et al.*, 2003; Kääb and Weber, 2004). The glacier forefield extends in elevation from 2650 m to 2900 m a.s.l. In the upper part of the cirque, from 2900 m to 3080 m a.s.l., a remnant of the former Muragl glacier exists (as of 2004; Figures 1 and 2). Temperature measurements in three shallow boreholes have shown that the Muragl glacier remnant consists of slightly cold ice (−0·5 to −1 °C) (Kneisel *et al.*, 1997). For the altitudinal range of the glacier forefield a mean annual air temperature of −2 to −4 °C can be inferred from two nearby mountain climate stations at 2250 m a.s.l. (−0·3 °C) and 3300 m a.s.l. (−6 °C). The bedrock consists of gneiss and mica schists.

At boreholes in the nearby Muragl rock glacier at an elevation of about 2550 m a.s.l. (i.e. 100 m lower than the forefield investigated but with similar topographic setting), negative ground temperatures close to 0 °C were measured (Arenson *et al.*, 2002; Vonder Mühll *et al.*, 2003).

The geomorphological mapping using a legend for high mountain geomorphology (cf. Kneisel *et al.*, 1998) was performed in 1996 and updated in August 1998 as recent morphodynamic processes such as active layer slides and small debris flows had exposed ground ice in the upper parts of the forefield. The detection of permafrost within this glacier forefield has been inferred using measurements of the bottom temperature of the winter snow cover (BTS) (Haeberli, 1992; Kneisel, 1999) and year-round near-surface temperature measurements as well as one-dimensional (1D) geoelectrical soundings (performed during 1996–1998, Kneisel, 1998, 1999). In summer 2002 and 2004 two-dimensional (2D) electrical resistivity tomography was applied.

Methods

Temperature measurements (BTS measurements and near-surface ground temperature logging)

Measurements of bottom temperatures of the winter snow cover (the so-called BTS method introduced by Haeberli, 1973) constitute a well established technique to map mountain permafrost. Hereby, a 3 m thermistor probe is pushed through the snow cover to the ground surface. An important boundary condition for the successful application of
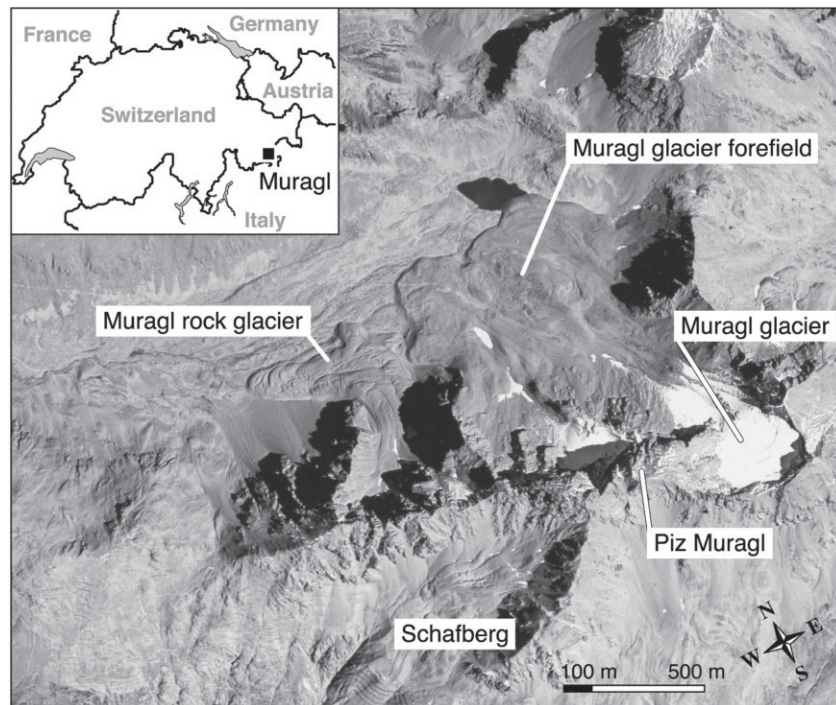
Figure 1. Aerial photograph of the Muragl valley with the glacier forefield under study. Inset: location of the study site within Switzerland. Aerial photograph taken by the swisstopo/flightservice on 7 September 1988.

Figure 2. Photograph of the Muragl glacier forefield. Muragl glacier remnant in the background to the top middle. Photograph taken on 12 August 2003.

this method is a sufficiently thick (at least 80 cm) snow cover. The snow cover, with its low thermal conductivity, insulates the ground from short-term fluctuations in air temperature. If the winter snow cover is sufficiently thick and surface melting is still negligible in mid- to late winter, the BTS values remain nearly constant and are mainly controlled by the heat transfer from the upper ground layers, which in turn is strongly influenced by the presence or absence of permafrost. Values obtained over permafrost are below −3 °C. Values between −2 and −3 °C represent the uncertainty range of the method and/or marginally active permafrost with thick active layer, which does not totally refreeze during winter. At permafrost-free sites or sites with inactive permafrost the measured values are above −2 °C.

In addition to spot measurements of the BTS, miniature temperature loggers were placed to record the BTS and year-round near-surface temperatures. From the latter data the mean annual ground surface temperature (MAGST) can be calculated. Permafrost exists if the MAGST is perennially below 0 °C (van Everdingen, 1998). Concerning the MAGST, the thermal offset, which is defined as the difference between mean annual temperature at the permafrost table and the mean annual ground surface temperature, has to be taken into account. Burn and Smith (1988) have suggested that permafrost may be in equilibrium, or aggrading, even under conditions where the mean annual ground surface temperature is slightly above 0 °C.

Geoelectrical surveys

Geophysical methods are particularly suitable for geomorphological investigations, since the knowledge of structure, layering and composition of the subsurface at different scales are key parameters for geomorphological problems. Among the different geophysical methods that are regularly applied, electrical resistivity tomography is considered as an important multifunctional method for research in periglacial geomorphology since a comprehensive characterization of the subsurface lithology can be obtained, a differentiation between genetic ice types is enabled in many cases according to the genetic/petrographic classification from Shumskii (1964) and the evolution of subsurface properties can be monitored. Congelation ice (interstitial and segregation ice), which is the predominant form of ground ice, shows lower resistivities that sedimentary ice, which is formed by snow–firn–ice metamorphosis. Characteristic values for sedimentary ice from temperate alpine firn zones are in the range of several MΩ m to more than 100 MΩ m (see, e.g., Reynolds, 1997). Resistivity values of frozen ground can vary over a wide range depending on the ice content (congelation ice), the temperature and the content of impurities. The dependence of resistivity on temperature is closely related to the amount of unfrozen water. Perennially frozen silt, sand, gravel or frozen debris with varying ice content shows resistivity values between 5 kΩ m and several hundred kΩ m (see, e.g., Haeberli and Vonder Mühll, 1996).

For this study the two-dimensional (2D) electrical surveys were performed using the Wenner and Wenner– Schlumberger configurations and an IRIS SYSCAL Junior Switch resistivity meter. The measured apparent resistivities are used to build up a vertical contoured section showing the lateral and vertical variation of resistivity over the section. The conventional method of plotting the results for the interpretation is the so-called pseudosection, which gives an approximate image of the subsurface resistivity distribution. The measured sets of apparent resistivities were inverted using the software package RES2DINV. Further details on different array geometries and data processing are given for instance by Reynolds (1997), Kneisel (2003b), Hauck and Vonder Mühll (2003). A deeper insight into the application of electrical resistivity tomography on different periglacial landforms is shown by Kneisel (2006).

As many as 45 2D resistivity surveys have been performed in 2002 and 2004 using parallel, overlapping and perpendicular profiles to cross-check the quality of the measurements and enhance the interpretation of the obtained results. Through this high number of survey profiles undertaken within a small area, the subsurface resistivity distribution was mapped and from this the permafrost distribution and characteristics were inferred.

Photogrammetry

Surface displacements for the glacier forefield were measured on the basis of digitized aerial photography of approximately 1:6000 scale taken on 7 September 1981 and on 23 August 1994. Digital terrain models (DTMs) of 1981 and 1994 were computed from photogrammetric stereo models using standard procedures of digital photogrammetry (Kääb and Vollmer, 2000; Kääb, 2005). Ortho-images of 1981 and 1994 were derived using these DTMs, the original digitized imagery and the image orientation calculated from precise ground control points available for the site. DTM generation and ortho-image production were conducted within the software SOCET SET. Horizontal movements were measured with 10 m grid spacing using a digital cross-correlation technique between the multitemporal ortho-images (software CIAS; Kääb and Vollmer, 2000; Kääb, 2002).

The air photos are from the same flight strips, which cover the nearby Muragl rock glacier. For the latter, an extensive accuracy assessment was performed by Kääb and Vollmer (2000) using the same flight parameters as applied for this study. Thereby, accuracy for individual displacement measurements was estimated to be about

$0 \cdot 02$–$0 \cdot 03$ m a^{-1} root mean square. Due to the similar imaging and ground conditions, this finding can also be assumed to apply for the Muragl glacier forefield.

Results and Interpretation

Permafrost occurrence

The occurrence of fluted moraines and a push moraine provides geomorphological evidence of a complex thermal regime of the former Muragl glacier with cold marginal parts frozen to the bed and warm-based ice in more central parts where fluted moraines could develop (Kneisel *et al.*, 2000). In the upper parts of the cirque, close to the glacier remnant, partly debris covered ice (dead ice) is present. Recent geomorphodynamic processes in the steep upper slopes of the cirque include small debris flows and several slides related to the occurrence of ground ice (Figure 3).
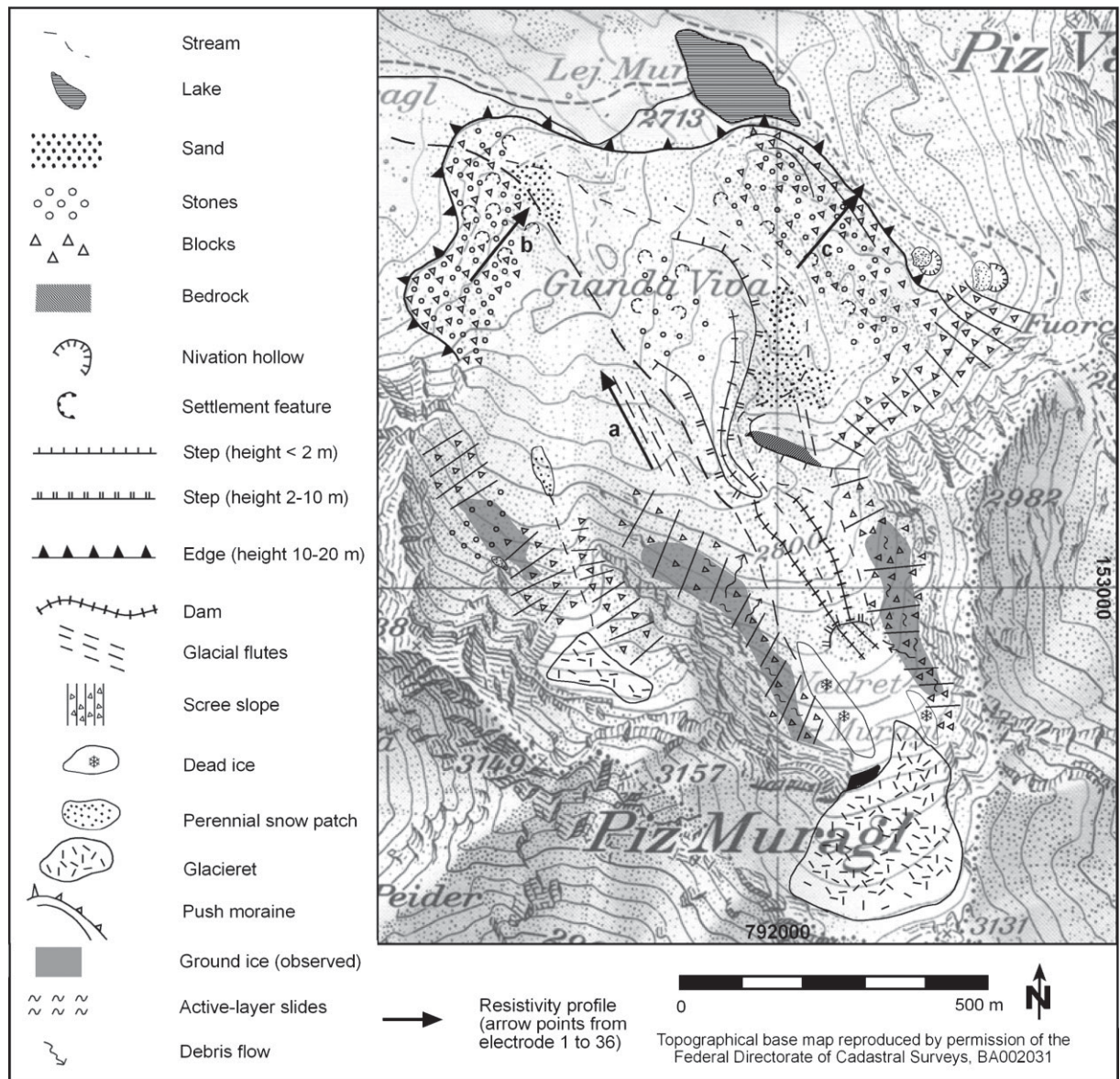

Figure 3. Geomorphological map of the Muragl glacier forefield.

The presence of permafrost at these sites impedes percolation of snowmelt and rain, leading to water saturation of the active layer, erosion and exposure of the ground ice. In places, the whole active layer is eroded and sediment has accumulated further downslope. Debris-covered ground ice is also found in the niche on the orographic left side with a small remnant of surface ice in the uppermost part. Towards the margins and in some central parts of the glacier forefield, settlement features are found in places that might be related to melting permafrost.

According to BTS measurements, performed in March 1998, the higher parts of the cirque between 2800 m and 2900 m a.s.l., and the outermost parts of the forefield close to the maximum glacier extent around AD 1850, are underlain by permafrost. In addition, on the orographic left side a band of measurements were recorded that are within the uncertainty range of the method (−2 to −3 °C). In the central parts of the forefield, permafrost is mapped as possible or improbable (Figure 4).
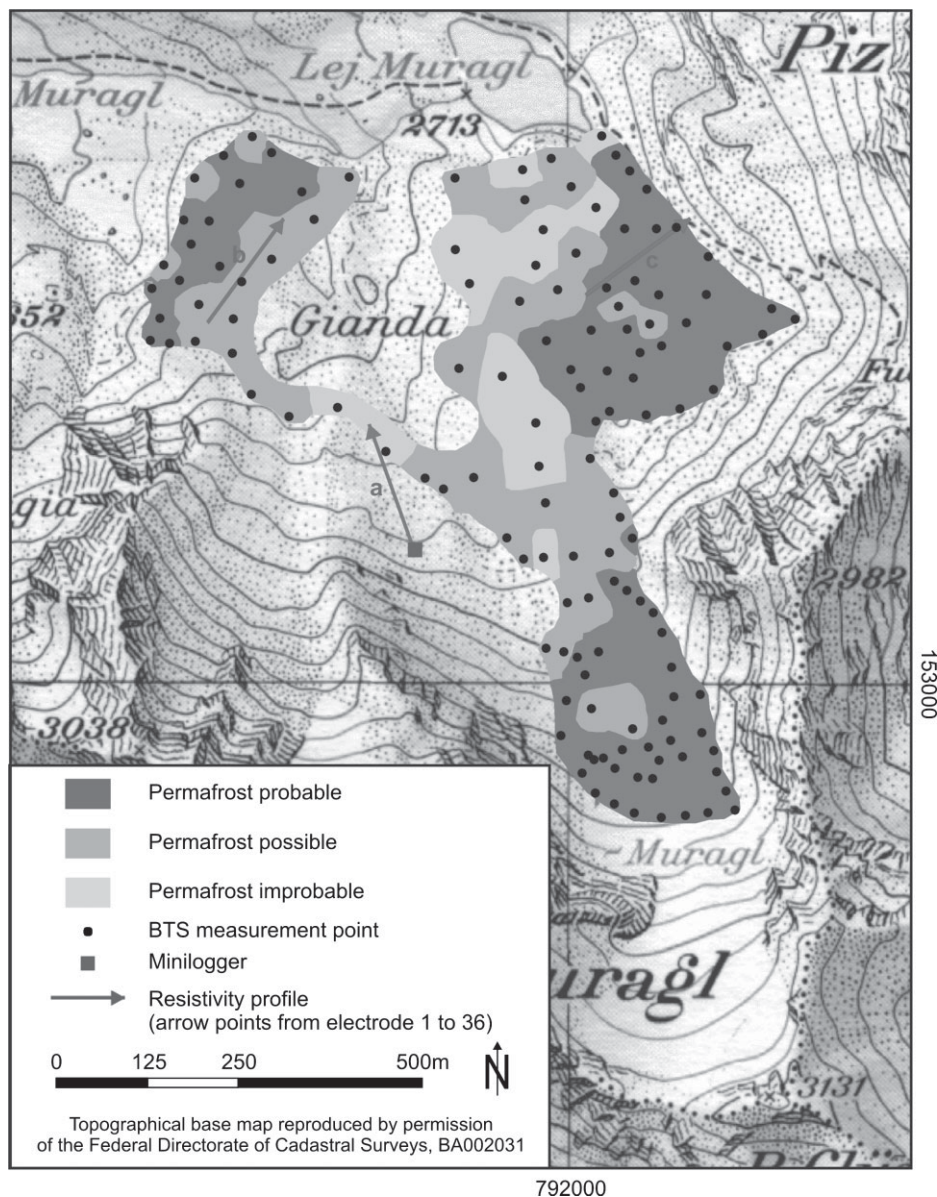

Figure 4. BTS measurements in the Muragl glacier forefield.

These results are supported by findings from 1D geoelectrical soundings and measured year-round near-surface ground temperatures for the period October 1997 until August 1999, which were recorded using seven miniature loggers, some of which were placed at the foot of steeper slopes, which are endangered by avalanches and thus not always accessible using the conventional BTS probe (Kneisel, 1999, 2003a).

The 2D geoelectrical surveys were focused on the outermost parts of the forefield, the orographic left side of the forefield close to the Muragl rock glacier, the push-moraine complex on the orographic right side and a more central part where glacial flutes have developed (Figure 3). The permafrost distribution in these parts of the Muragl glacier forefield as delineated through the 2D electrical resistivity surveys has been classified into three classes: low resistivity permafrost (<100 kΩ m), medium resistivity permafrost (>100 kΩ m) and high resistivity permafrost (>1 MΩ m). The latter can be considered as massive ground ice. The three classes are depicted as grey areas in Figure 7. These shaded areas are represented through several 2D resistivity surveys, some of which were arranged as crossing and/or perpendicular surveys in order to obtain more reliable results. Further permafrost occurrences are present in more central and upper parts of the forefield (not shown in Figure 7). The terrain sections between the shaded areas are either not represented to a sufficient level in the geophysical surveys or are considered as permafrost free according to the results of the 2D geoelectric measurements. One typical electrical resistivity tomogram representing each of the three classes is given (Figure 5(a)–(c)). The locations of the profiles are given in Figures 3, 4 and 7.

In the upper parts of the Wenner survey in Figure 5(a) down to the middle parts, an anomaly is detected, which can be interpreted as shallow permafrost. The resistivities are fairly low, which could indicate a low ice content. However, with the special conditions in glacier forefields, permafrost occurrences can be assumed to be shallow, 'warm' and thus rich in unfrozen water, which can explain the comparatively low apparent resistivity values (Kneisel, 2003a, 2004). The comparatively thick active layer in the central part of the survey could be evidence of degrading permafrost at this site. The third layer is interpreted as the unfrozen ground underneath the permafrost (glacial till or bedrock). A differentiation between bedrock and glacial till in the investigated forefield is made difficult by the fact that dry glacial till shows similar resistivities as the bedrock, with values around 2–4 kΩ m. Through one-dimensional sounding, similar thickness of the active layer and depth of the permafrost were obtained (Kneisel, 1999).

In order to assess ground thermal conditions, one of the temperature loggers was placed in the upper parts of the survey line (Figure 6). The logger was obviously covered by a thick enough snow cover, as there are no high-frequency variations visible in the graph and the values decrease gradually until the final more or less constant temperature is reached in the mid- to late-winter months. Thus, the bottom temperatures of the snow cover can be analysed according to the three distinguished BTS classes. From the beginning of May an increase of the temperatures to 0 °C is visible; in the following weeks the temperatures remain constant around 0 °C (zero curtain). This feature is typical for mountain permafrost with dry freezing in autumn without development of a zero curtain and wet thawing in spring with pronounced zero curtain.

In both winter periods the logger recorded BTS values that indicate permafrost. Mean annual ground surface temperatures could be calculated for the period 1 October 1997 to 30 September 1998 and 1 August 1998 to 31 July 1999. The results with negative mean annual ground temperatures (−0·85 and −1·34 respectively) point to permafrost favourable conditions during the measurement period.

The survey presented in Figure 5(b) was performed on the outermost parts of the forefield on the orographic left side close to the maximum glacier extent around AD 1850, where BTS measurements point to the presence of permafrost (Figure 4). The pseudosection of resistivities against depth shows a large highly resistive anomaly extending from the middle to the right side of the profile, indicating a permafrost body. From the range of resistivities, it can be concluded that the subsurface consists of ice-rich layers and that the ice content is decreasing with depth. The active layer appears to be of variable thickness. The layer underneath the permafrost is interpreted as unfrozen glacial till or bedrock at a depth of 20–25 m.

The survey presented in Figure 5(c) was performed on the push-moraine complex on the orographic right side (Figure 3). A large highly resistive anomaly is detected extending over the left side of the survey area, indicating a massive ice body. From the range of resistivities, it can be concluded that the ice body consists of polygenetic ice, i.e. sedimentary ice from a firnification process (typical glacier ice) and segregation ice (typical permafrost ice from ground freezing).

Surface velocity field

Horizontal surface displacements of 10 m spacing have been measured by matching aerial photographs from 7 September 1981 with those from 23 August 1994. The results revealed three zones of significant movement. Zone a (Figure 8) shows surface speeds of up to 0·55 m a^{-1}. The front is advancing horizontally by approximately 0·17 m a^{-1},
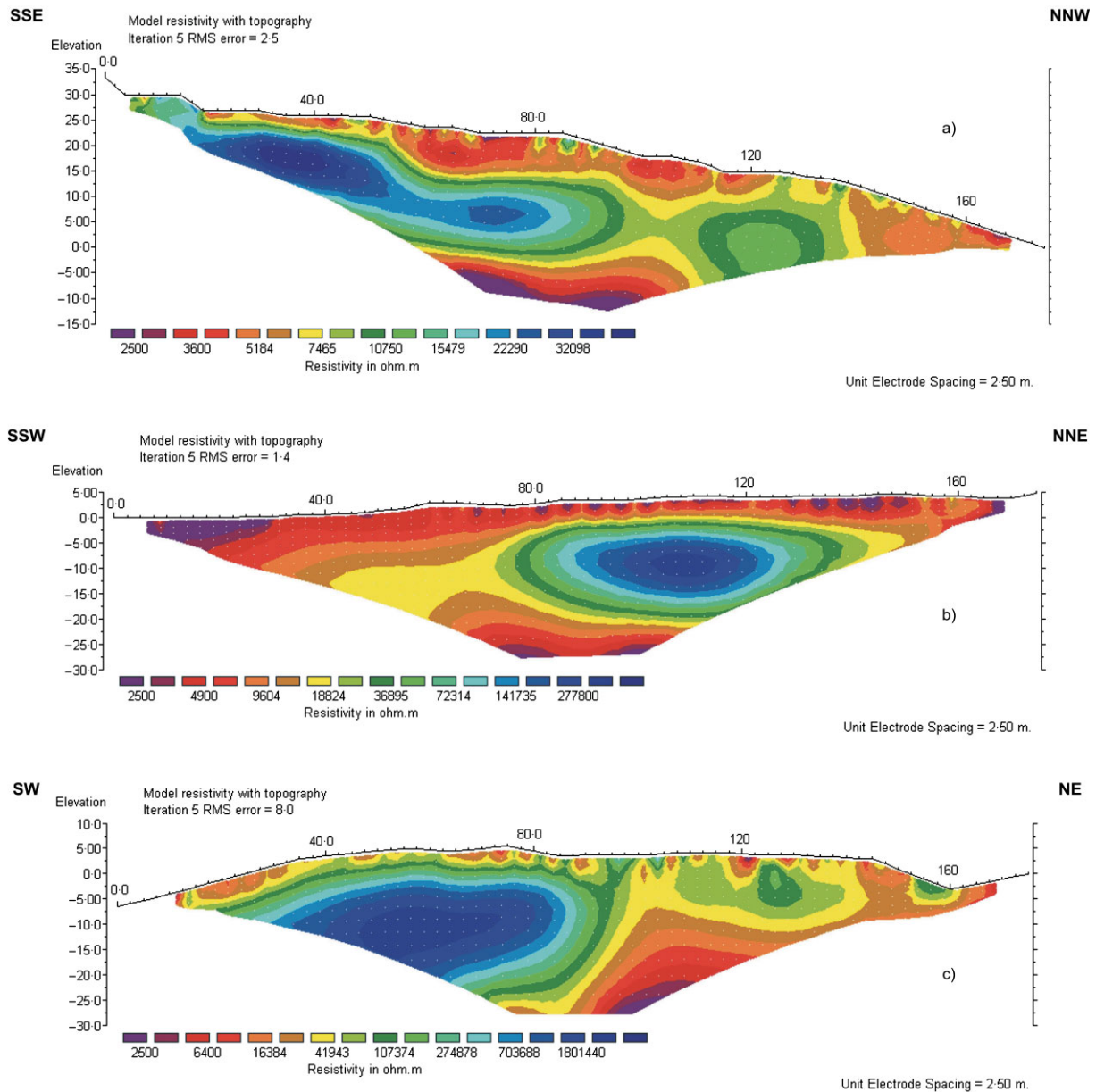
Figure 5. Electrical resistivity tomograms representing the 'low resistivity class' (a), the 'medium resistivity class' (b) and the 'high resistivity class' (c). This figure is available in colour online at www.interscience.wiley.com/journal/espl

even more in parts, as found by image and DTM comparison. No significant supply of frozen debris by creep from the upper parts of the glacier forefield can be detected.

The same applies for zone b. There, horizontal movement amounts to 0·16 m a^{-1}. A potential advance of the corresponding front is within the measurement accuracy. Near Lake Muragl in zone c, the location of a Holocene push moraine, movement of the order of 0·15 m a^{-1} can be observed. In all zones described, the creep direction follows the direction of steepest slope. For the area of the push moraine this implies a reverse creep against the flow direction of the former glacier. Beside zones a–c, no significant movement during 1981 to 1994 was detected on the Muragl glacier forefield.

Figure 6. Mean daily near-surface temperatures (Oct. 1996–Aug. 1999).

Discussion

The patchy permafrost distribution pattern within the Muragl glacier forefield is determined by several factors, including local variability of the energy balance, sediment characteristics, snow cover distribution and duration, aspect and the former glacier distribution and thermal regime. Recent and modern permafrost dynamics comprise aggradation, degradation and permafrost creep respectively.

Geomorphological evidence for a complex thermal regime of the former glacier with cold marginal parts frozen to the bed and warm-based ice in more central parts is provided through the occurrence of the well developed push moraine and the fluted moraines (Haeberli, 1983; Kneisel *et al.*, 2000). The shallow permafrost occurrences in the latter areas as derived by geoelectrical surveys are interpreted as a new formation after the retreat of the temperate surface ice (cf. Figure 5(a)). The low resistivity values are interpreted as permafrost occurrences that consist of a large amount of frozen material of different grain sizes rather than a saturated or supersaturated massive ice layer (Kneisel, 2003a). This interpretation is now supported by results of shallow borehole drilling, which was recently performed, showing loose glacial sediments down to a depth of 8 m. Furthermore, no significant movement could be detected by the photogrammetric analyses in this part of the glacier forefield. In contrast, the horizontal surface displacement rates – most of them surprisingly high – in zones a–c (Figure 8) seem, for the most part, to reflect a process of local material mobilization, and not so much the result of material supply over longer distances. The results correspond well with the geoelectrical surveys performed in the area and the BTS measurements of 1985 (Haeberli, 1992) and 1996 (Kneisel, 1999), which suggest that zones a–c are underlain by permafrost. Based on the findings of the geoelectrical surveys and the surface displacement measurements, zone a can be described as a transition form of talus- and moraine-derived rock glacier.

The comparatively large ratio between advance rate and surface velocity at the front of zone a points to little volume loss by ice melt-out and, thus, to a relatively small overall ice content of the body (Kääb and Kneisel, 2006). Morphological expression of permafrost creep, as observed in the field, is indicated by the steep front. However, no furrow and ridge systems can be found because of the dominant extending flow regime as compared to the adjacent Muragl rock glacier, showing similar surface speed of about 0·50 m a^{-1} but also compressive flow patterns. Strong
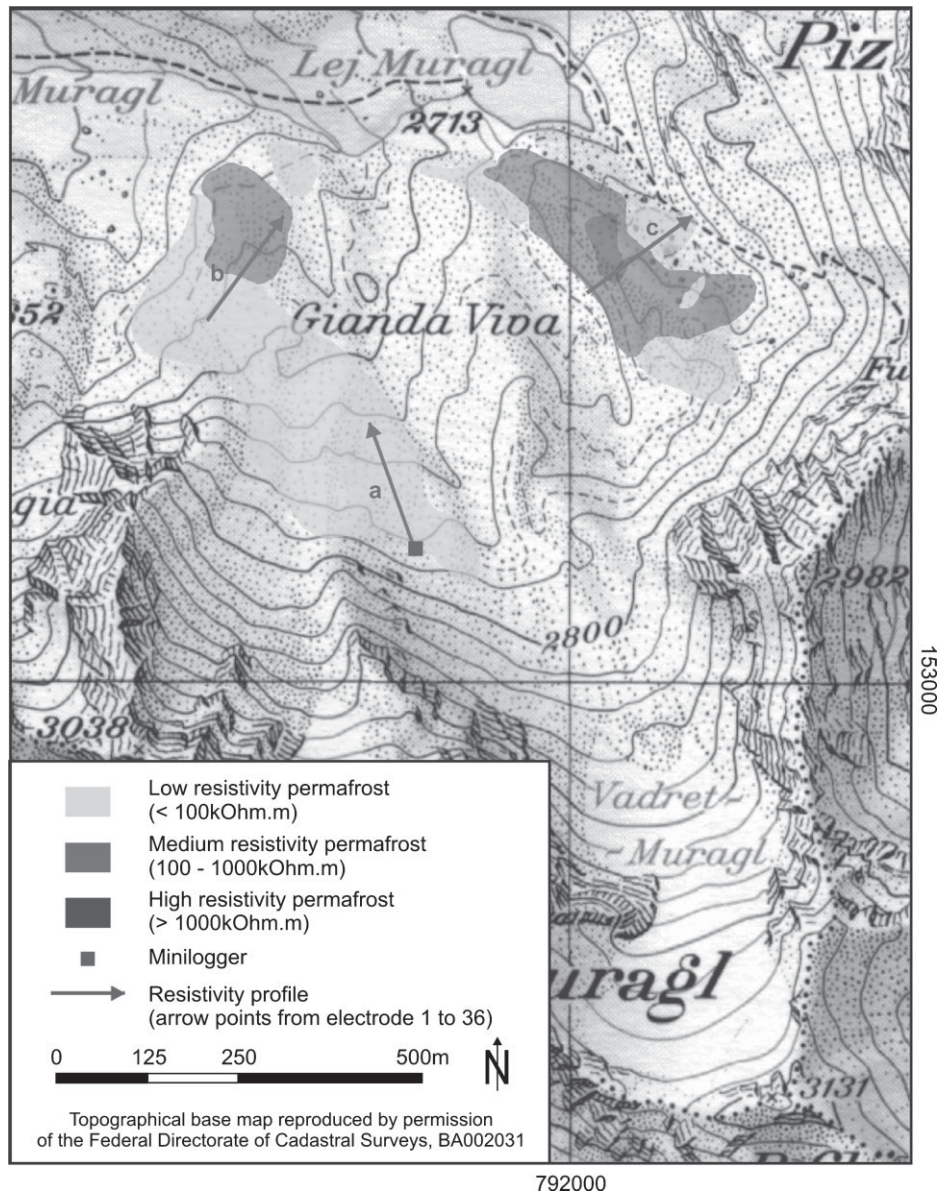
Figure 7. Ground ice/permafrost occurrence in the marginal parts of the Muragl glacier forefield as delineated from 2D electrical resistivity surveys.

oversteepening of the front indicates that the movement is restricted, for the most part, to an approximately 10–15 m deep surface layer (cf. the front of Gruben rock glacier in the work of Kääb and Reichmuth, 2005). This interpretation compares well with findings from the 2D resistivity surveys, which indicate low-resistivity permafrost in most parts of zone a. Low resistivities in this permafrost environment can be interpreted in terms of warm permafrost, i.e. close to 0 °C. The associated high unfrozen water content could result in such low resistivities even in the presence of permafrost lenses with rather high ice contents (Kneisel, 2003a, 2004). 'Warm' permafrost temperatures might explain the considerable movement compared with the low slope angle, for most zones not exceeding 15° (Kääb et al., 2002, in press).

One-dimensional geoelectrical soundings for zone b gave indications of comparable thin and/or melting permafrost, with an active layer of 2–5 m thickness (Kneisel, 1999). The results of the more recent 2D surveys indicate medium resistivity permafrost of considerable horizontal extent with variable active layer depth in this area. Geomorphological
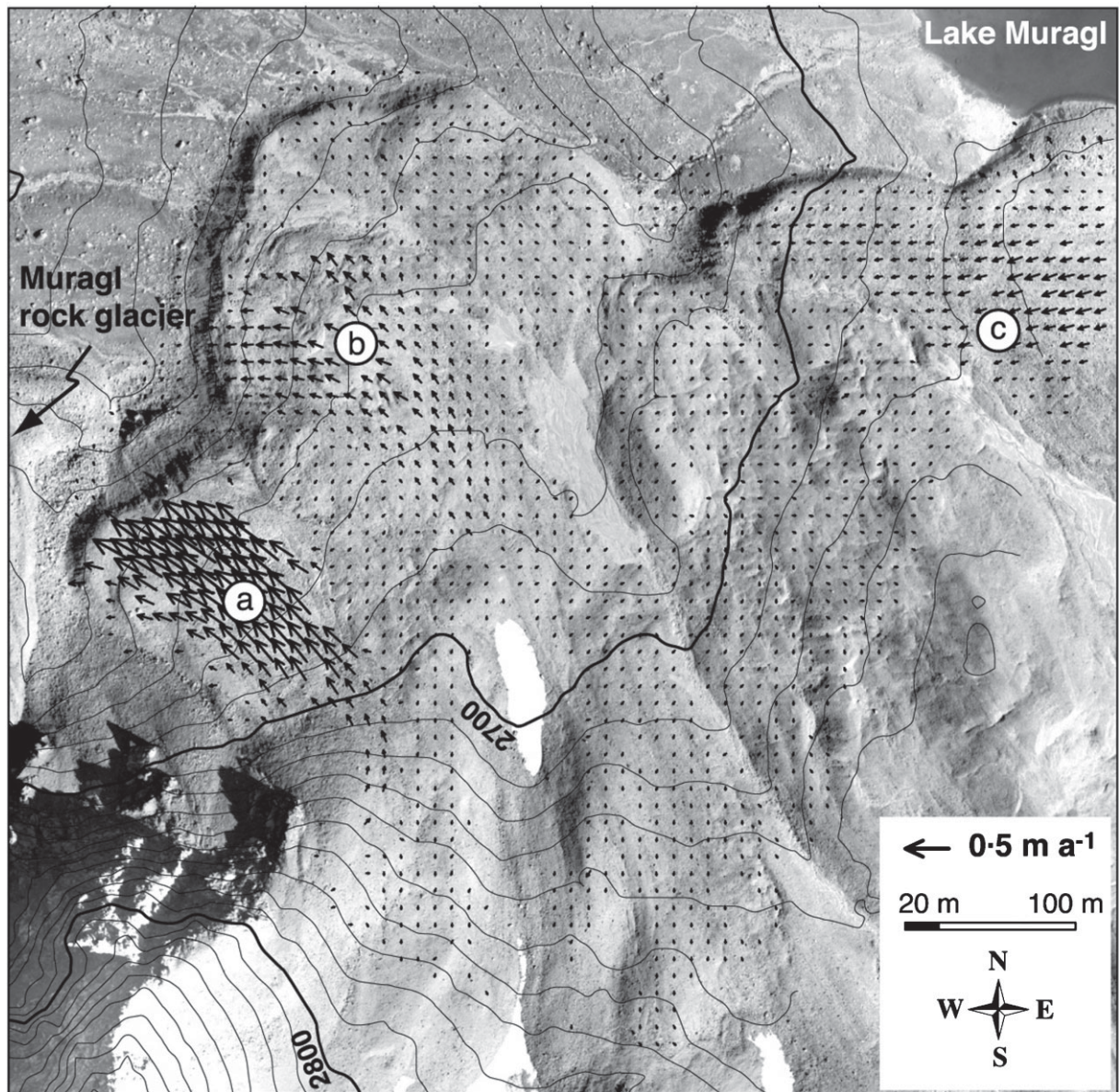
Figure 8. Horizontal surface displacements 1981–1994 on a section of the Muragl glacier forefield. For letters a–c refer to the text.

hints for such a scheme of locally active and inactive permafrost could be the small-scale settlement features which can be found in this area of the forefield and could point to degrading permafrost.

Zone c is interpreted as part of a push-moraine complex (Haeberli, 1979, 1983). Thus some downslope creep – back to the area covered by the Little Ice Age glacier – seems possible. The indication of permafrost in that zone from BTS measurements (Haeberli, 1992; Kneisel, 1999) is also supported by the 2D resistivity surveys, which show a large area of medium-resistivity and in parts even high-resistivity permafrost within the main body of the moraine complex. Geoelectrical soundings point to ice-rich frozen ground in parts of the proximal side of the push moraine, consisting of polygenetic or even sedimentary origin as can be delineated from the range of resistivities, which exceed 1 MΩ m. The rest of the push moraine still shows resistivities higher than 100 kΩ m. In this context it should be emphasized that occasionally a close coexistence of different ice types, as deduced through geoelectrical surveys, can be observed in glacial and periglacial environments. Ice of polygenetic origin, but also a close coexistence of high-resistivity

sedimentary ice (typical of temperate alpine firn zones) and medium- or even low-resistivity subsurface ice is possible (Kneisel, 1999, 2003a).

In many studies in mountain environments the application of two different geophysical methods and the cross-checking of their results are applied or at least recommended for a more sophisticated characterization of the subsurface structure (e.g. Ikeda and Matsuoka, 2002; Kneisel and Hauck, 2003; Maurer *et al.*, 2003; Bucki *et al.*, 2004; Hauck *et al.*, 2004). In areas with close proximity of sediment bodies underlain by (ice-rich) permafrost we suggest the combination of geophysics for detailed mapping in conjunction with photogrammetry. Hereby, electrical resistivity imaging is considered as an important multi-functional geophysical method for research in periglacial permafrost related environments. Joint application with measurements of surface displacements offers a promising tool for investigating periglacial landforms related to ice-rich permafrost for a more comprehensive characterization of permafrost characteristics and geomorphological interpretation of recent and modern periglacial morphodynamics.

The integrative analysis shows that the occurrence of coherent movement patterns indicating cohesive flow with larger-scale stress transmission is intimately coupled with the existence of subsurface ice. This subsurface ice can have polygenetic origin as reflected in variable electrical DC resistivity but obviously depends on conditions of negative ground temperatures or permafrost conditions respectively (cf. Haeberli, 2000).

Future research will include geophysical mapping of permafrost at other sites in conjunction with the corresponding measurements of the surface velocity field to link the kinematic behaviour to the subsurface properties.

Conclusions

Geomorphological observations, near-surface temperature measurements, geoelectrical soundings and photogrammetric measurements of surface displacements on the Muragl glacier forefield were used to obtain an integrative analysis of a highly complex glacial and periglacial landform. A valuable aspect of modern geophysical techniques and their application in geomorphology is the ability to image the subsurface. In this application, a coherent surface velocity field is viewed as a proxy for frozen debris with a slope steep enough, and an ice content high and long-lasting enough, to allow for significant ductile deformation of the material.

The agreement between the photogrammetric measurements and geophysical surveys presented here demonstrates that the investigation of surface kinematics in cold mountain environments can be a suitable tool to detect surface deformation as a proxy for ice-containing permafrost. The combined approach allows a better understanding of the landscape evolution influenced by complex glacier–permafrost relationships as well as the recent interplay between ice content and slope deformation. Hereby, integrative analyses have the potential to improve the understanding of permafrost-related periglacial landforms, which may exhibit active (supersaturated with ice and creeping), inactive (degrading ice and almost no creeping) and relict (ice-free, no creeping) sediment bodies in close proximity.

Acknowledgements

References

Arenson L, Hoelzle M, Springman S. 2002. Borehole deformation measurements and internal structure of some rock glaciers in Switzerland. *Permafrost and Periglacial Processes* **13**: 117–135.

Berthling I, Etzelmüller B, Eiken T, Sollid JL. 1998. Rock glaciers on Prins Karls Forland, Svalbard, I: internal structure, flow velocity and morphology. *Permafrost and Periglacial Processes* **9**: 135–145.

Bucki AK, Echelmeyer KA. 2004. The flow of Fireweed rock glacier, Alaska, USA. *Journal of Glaciology* **50**(168): 76–86.

Bucki AK, Echelmeyer KA, MacInnes S. 2004. The thickness and internal structure of Fireweed rock glacier, Alaska, USA, as determined by geophysical methods. *Journal of Glaciology* **50**(168): 67–75.

Burn CR, Smith CAS. 1988. Observations of the 'thermal offset' in near-surface mean annual ground temperatures at several sites near Mayo, Yukon Territory, Canada. *Arctic* **41**(2): 99–104.

Delaloye R. 2004. *Contribution à lEtude du Pergelisol de Montage en Zone Marginale*, PhD thesis. Département de Géosciences, Géographie–Géomorphologie, Université de Fribourg.

Haeberli W. 1973. Die Basis Temperatur der winterlichen Schneedecke als möglicher Indikator für die Verbreitung von Permafrost. *Zeitschrift für Gletscherkunde und Glazialgeologie* **9**(1/2): 221–227.

Haeberli W. 1979. Holocene push-moraines in alpine permafrost. *Geografiska Annaler* **61**A: 43–48.

Haeberli W. 1983. Permafrost–glacier relationships in the Swiss Alps – today and in the past. *Proceedings, Fourth International Conference on Permafrost, Fairbanks, Alaska*. National Academy Press: Washington, DC; 415–420.

Haeberli W. 1992. Possible effects of climatic change on the evolution of Alpine permafrost. In *Greenhouse-Impact on Cold-Climate Ecosystems and Landscapes*, Boer M, Koster E (eds). *Catena Supplement* **22**: 23–35.

Haeberli W. 2000. Modern research perspectives relating to permafrost creep and rock glaciers: a discussion. *Permafrost and Periglacial Processes* **11**: 290–293.

Haeberli W, Vonder Mühll D. 1996. On the characteristics and possible origins of ice in rock glacier permafrost. *Zeitschrift für Geomorphologie N.F. Supplement* **104**: 43–57.

Hauck C, Isaksen K, Vonder Mühll D, Sollid JL. 2004. Geophysical surveys designed to delineate the altitudinal limit of mountain permafrost: an example from Jotunheimen, Norway. *Permafrost and Periglacial Processes* **15**: 191–205.

Hauck C, Vonder Mühll D. 2003. Evaluation of geophysical techniques for application in mountain permafrost studies. In *Geophysical Methods in Geomorphology*, Schrott L, Hoerdt A, Dikau R (eds). *Zeitschrift für Geomorphologie Supplement* **132**: 161–190.

Hoelzle M, Wagner S, Kääb A, Vonder Mühll D. 1998. Surface movement and internal deformation of icerock mixtures within rock glaciers in the Upper Engadin, Switzerland. In *Proceedings of the Seventh International Conference on Permafrost, Yellowknife, Canada*, Collection Nordicana, Université Laval; 465–472.

Ikeda A, Matsuoka N. 2002. Degradation of talus-derived rock glaciers in the Upper Engadin, Swiss Alps. *Permafrost and Periglacial Processes* **13**: 145–161.

Ikeda A, Matsuoka N, Kääb A. 2003. A rapidly moving small rock glacier at the lower limit of the mountain permafrost belt in the Swiss Alps. *Proceedings of the Eighth International Conference on Permafrost, Zurich*, Vol. 1. Balkema; 455–460.

Isaksen K, Ødegard RS, Eiken T, Sollid JL. 2000. Composition, flow and development of two tongue-shaped rock glaciers in the permafrost of Svalbard. *Permafrost and Periglacial Processes* **11**: 241–257.

Kääb A. 2002. Monitoring high-mountain terrain deformation from air- and spaceborne optical data: examples using digital aerial imagery and ASTER data. *ISPRS Journal of Photogrammetry and Remote Sensing* **57**(1/2): 39–52.

Kääb A. 2005. Remote sensing of mountain glaciers and permafrost creep. *Schriftenreihe Physische Geographie* **48**.

Kääb A, Frauenfelder R, Roer I. in press. On the response of rockglacier creep to surface temperature increase. *Global and Planetary Change*. DOI: 10.1016/j.gloplacha.2006.07.005

Kääb A, Isaksen K, Eiken T, Farbrot H. 2002. Geometry and dynamics of two lobe-shaped rock glaciers in the permafrost of Svalbard. *Norwegian Journal of Geography* **56**: 152–160.

Kääb A, Kneisel C. 2006. Permafrost creep within a recently deglaciated glacier forefield: Muragl, Swiss Alps. *Permafrost and Periglacial Processes* **17**: 79–85.

Kääb A, Reichmuth T. 2005. Advance mechanisms of rock glaciers. *Permafrost and Periglacial Processes* **16**: 187–193.

Kääb A, Vollmer M. 2000. Surface geometry, thickness changes and flow fields on creeping mountain permafrost: automatic extraction by digital image analysis. *Permafrost and Periglacial Processes* **11**: 315–326.

Kääb A, Weber M. 2004. Development of transverse ridges on rock glaciers: field measurements and laboratory experiments. *Permafrost and Periglacial Processes* **15**: 379–391.

Kneisel C. 1998. Occurrence of surface ice and ground ice/permafrost in recently deglaciated glacier forefields, St. Moritz area, Eastern Swiss Alps. In *Proceedings of the Seventh International Conference on Permafrost, Yellowknife, Canada*, Collection Nordicana, Université Laval; 575–581.

Kneisel C. 1999. Permafrost in Gletschervorfeldern – eine vergleichende Untersuchung in den Ostschweizer Alpen und Nordschweden, PhD thesis. *Trierer Geographische Studien* **22**.

Kneisel C. 2003a. Permafrost in recently deglaciated glacier forefields – measurements and observations in the eastern Swiss Alps and northern Sweden. *Zeitschrift für Geomorphologie* **47**: 289–305.

Kneisel C. 2003b. Electrical resistivity tomography as a tool for geomorphological investigations – some case studies. In *Geophysical Methods in Geomorphology*, Schrott L, Hoerdt A, Dikau R (eds). *Zeitschrift für Geomorphologie Supplement* **132**: 37–49.

Kneisel C. 2004. New insights into mountain permafrost occurrence and characteristics in glacier forefields at high altitude through the application of 2D resistivity imaging. *Permafrost and Periglacial Processes* **15**: 221–227.

Kneisel C. (2006). Assessment of subsurface lithology in mountain environments using 2D resistivity imaging. *Geomorphology* **80**: 32–44.

Kneisel C, Haeberli W, Baumhauer R. 1997. Aktuelle Gletscherveränderungen und Permafrostverbreitung in den Ostschweizer Alpen, Oberengadin/St. Moritz. *Trierer Geographische Studien* **16**: 19–32.

Kneisel C, Haeberli W, Baumhauer R. 2000. Comparison of spatial modelling and field evidence of glacier/permafrost relations in an alpine permafrost environment. *Annals of Glaciology* **31**: 269–274.

Kneisel C, Hauck C. 2003. Multi-method geophysical investigation of a sporadic permafrost occurrence. In *Geophysical Methods in Geomorphology*, Schrott L, Hoerdt A, Dikau R (eds). *Zeitschrift für Geomorphologie Supplement* **132**: 145–159.

Kneisel C, Lehmkuhl F, Winkler S, Tressel E, Schröder H. 1998. Legende für geomorphologische Kartierungen in Hochgebirgen (GMK Hochgebirge). *Trierer Geographische Studien* **18**.

Konrad SK, Humphrey NF, Steig EJ, Clark DH, Potter N Jr, Pfeffer WT. 1999. Rock glacier dynamics and paleoclimatic implications. *Geology* **27**(12): 1131–1134.

Lambiel C, Delaloye R. 2004. Contribution of real-time kinematic GPS in the study of creeping mountain permafrost: examples from the Western Swiss Alps. *Permafrost and Periglacial Processes* **15**: 229–241.

Lugon R, Delaloye R, Serrano E, Reynard E, Lambiel C, Gonzalez-Trueba JJ. 2004. Permafrost and Little Ice Age glacier relationships, Posets Massif, Central Pyrenees, Spain. *Permafrost and Periglacial Processes* **15**: 207–220.

Maisch M, Haeberli W, Frauenfelder R, Kääb A. 2003. Lateglacial and Holocene evolution of glaciers and permafrost in the Val Muragl, Upper Engadine, Swiss Alps. In *Proceedings of the Eighth International Conference on Permafrost, Zurich*, Vol. 2. Balkema; 717–722.

Maurer HR, Springman SM, Arenson LU, Musil M, Vonder Mühll D. 2003. Characterisation of potentially unstable mountain permafrost – a multidisciplinary approach. In *Proceedings of the Eighth International Conference on Permafrost, Zurich*, Vol. 2. Balkema; 741–746.

Potter N, Steig EJ, Clark DH, Speece MA, Clark GM, Updike AB. 1998. Galena Creek rock glacier revisited – new observations on an old controversy. *Geografiska Annaler* **80A**(3/4): 251–265.

Reynard E, Lambiel C, Delaloye R, Devaud G, Baron L, Chapellier D, Marescot L, Monnet R. 2003. Glacier/permafrost relationships in forefields of small glaciers (Swiss Alps). In *Proceedings of the Eighth International Conference on Permafrost, Zurich*, Vol. 2. Balkema; 947–952.

Reynolds JM. 1997. *An Introduction to Applied and Environmental Geophysics*. Wiley: Chichester.

Shumskii PA. 1964. *Principles of Structural Glaciology*. Dover: New York.

van Everdingen RO. 1998. *Multi-Language Glossary of Permafrost and Related Ground-Ice Terms*. University of Calgary: Calgary.

Vonder Mühll D, Arenson L, Springman S. 2003. Temperature conditions in two Alpine rock glaciers. In *Proceedings of the Eighth International Conference on Permafrost, Zurich*, Vol. 2. Balkema; 1195–1200.

Vonder Mühll D, Schmid W. 1993. Geophysical and photogrammetrical investigation of rock glacier Muragl I, Upper Engadin, Swiss Alps. In *Proceedings of the Sixth International Conference on Permafrost, Zurich*, Vol. 1. Bejing; 214–219.